Available online at www.sciencedirect.com
ScienceDirect
Journal of Solid State Chemistry 181 (2008) 957–963
JOURNAL OF SOLID STATE CHEMISTRY
www.elsevier.com/locate/jssc

Microwave-induced synthesis of highly dispersed gold nanoparticles within the pore channels of mesoporous silica

Jinlou Gu, Wei Fan, Atsushi Shimojima, Tatsuya Okubo*

Department of Chemical System Engineering, The University of Tokyo, 7-3-1 Hongo, Bunkyo-ku, Tokyo 113-8656, Japan

Received 13 December 2007; received in revised form 30 January 2008; accepted 31 January 2008
Available online 9 February 2008

Abstract

Highly dispersed gold nanoparticles have been incorporated into the pore channels of SBA-15 mesoporous silica through a newly developed strategy assisted by microwave radiation (MR). The sizes of gold are effectively controlled attributed to the rapid and homogeneous nucleation, simultaneous propagation and termination of gold precursor by MR. Diol moieties with high dielectric and dielectric loss constants, and hence a high microwave activation, were firstly introduced to the pore channels of SBA-15 by a simple addition reaction between amino group and glycidiol and subsequently served as the reduction centers for gold nanoparticles. Extraction of the entrapped gold from the nanocomposite resulted in milligram quantities of gold nanoparticles with low dispersity. The successful assembly process of diol groups and formation of gold nanoparticles were monitored and tracked by solid-state NMR and UV–vis measurements. Characterization by small angle X-ray diffraction (XRD) and transmission electron microscopy (TEM) indicated that the incorporation of gold nanoparticles would not breakup the structural integrity and long-range periodicity of SBA-15. The gold nanoparticles had a narrow size distribution with diameters in the size range of 5–10 nm through TEM observation. The average particles size is 7.9 nm via calculation by the Scherrer formula and TEM measurements. Nitrogen adsorption and desorption isotherms gave further evidence that the employed method was efficient and gold nanoparticles were successfully incorporated into the pore channels of SBA-15.

Keywords: Gold; Nanoparticles; Microwave radiation; Mesoporous silica; SBA-15

1. Introduction

The synthesis of metallic nanostructured materials has become the focus of intensive researches, as these materials have superior optical, electronic and catalytic properties, which differ significantly from their bulk counterparts [1,2]. However, the morphology, dimension and size control of the synthesized nanomaterials is still a challenge [3]. It is generally accepted that the preparation of nanostructured metals in a preformed space [4], such as organic soft template [5] or inorganic framework hard template [6], provides a simple, high-throughput and cost-effective procedure. Recently, mesoporous silica [7,8], such as well-known SBA-15 molecular sieves, has been used as molds for the growth of different nanostructured metals in order to control their size, shape and organization [9]. Moreover, these composites themselves consisted of mesoporous materials (MMs) with noble metals encapsulated also possess peculiar and fascinating properties [10–14]. A lot of methods [15–19] such as aqueous impregnation [20], ion-exchange [21], just to name a few, have been employed to incorporate metallic nanoparticles into MMs. Most of these methods involved the high-temperature reduction process, which was somewhat limited by the tendency of metal to agglomerate on the outside surface of the host MMs due to the rapid and enhanced diffusion [22]. It was also difficult to control the growth of the nanomaterials, resulting in uncontrolled dimensions of the synthesized nanostructures such as nanoparitcles, nanorods, or nanowires [23]. The low-temperature reduction approach was also used to prepare the highly dispersed metallic nanoparticles within the pore channels of MMs [24], but the complicated multi-step procedures had to be employed

*Corresponding author. Fax: +81 3 58003806.
E-mail address: okubo@chemsys.t.u-tokyo.ac.jp (T. Okubo).

0022-4596/$ - see front matter © 2008 Elsevier Inc. All rights reserved.
doi:10.1016/j.jssc.2008.01.039

to introduce reduction centers into the inner void space of the host materials, which seemed unfavorable to scale-up the synthesis of the target metallic nanoparticles. Therefore, development of a mild and highly efficient strategy for the synthesis of the target host–guest mesoporous composites is still highly desired.

Recently, many successes have been reported in using microwave radiation (MR) to assist the synthesis of highly pure metallic nanoparticles with narrow size distribution [25,26]. Microwave heating through dielectric losses is fast, uniform and energy efficient. The greatest advantage of MR is that it can heat a substance directly, leading to a more homogeneous nucleation and shorter crystallization time compared to conventional heating [27]. This is beneficial to the formation of uniform metallic colloids [28,29]. It is also reported that MR is subject to transmit mesoporous silica framework without energy loss [30]. Since microwave activation groups are easy to be introduced into the pore channels of mesoporous silica with high specific surface area for the heterogeneous nucleation and growth of metallic nanoparticles, the smaller and uniformly dispersed metallic nanoparticles within MMs could be rapidly obtained upon MR. In the current investigation, we propose a new and simple strategy to prepare SBA-15 with highly dispersed metallic nanoparticles assisted by MR. We took gold nanoparticles as a specific example attributed to their wide application potentials such as in heterogeneous catalysis [2,11] or nonlinear optic fields [1], although the method is universal and can be easily extended to the other metals.

2. Experimental

2.1. Preparation of SBA-15 mesoporous silica

In a typical run, 4 g of Pluronic P123 ($EO_{20}PO_{70}EO_{20}$, BASF) was dissolved in 30 g of distilled water mixed with 120 g of 2 M HCl solution. The resulting mixture was stirred at 308 K to obtain a clear and homogeneous solution, to which 8.5 g of tetraethoxysilane (TEOS, Wako) was gradually added under vigorous stirring for 20 h at 311 K. The mixture was subsequently heated at 373 K for 2 days. The resultant solid was filtered off and then extensively washed with deionized water. Drying at 393 K for 24 h yielded the as-synthesized SBA-15 [7]. The surfactant template was removed by solvent extraction using ethanol with a little concentrated HCl added under refluxing for 3 days.

2.2. Preparation of SBA-15 with diol modified

The resultant SBA-15 (1 g) without surfactant was extensively washed with ethanol and deionized water and dried at 423 K for 24 h to remove the adsorbed water and then put into 100 mL of dried toluene solution which was treated over zeolite 4A in advance. After half an hour, 2 mL of aminopropyltrimethoxysilane (APS, Wako) was poured into the above toluene solution under a nitrogen atmosphere and then refluxed for 12 h to obtain MMs with $-NH_2$ groups modified [31]. The product was separated by filtration and then dried at 373 K in vacuo for 24 h. The 0.5 g of the above amino-groups modified SBA-15 sample was dropped slowly into 20 mL of glycidol solution under stirring with ice cooling, and then the mixture was reacted for 1 h at room temperature [32]. The final product was centrifuged and washed with water and ethanol solution for several times.

2.3. Preparation of SBA-15 with gold nanoparticles loaded and removal of mesoporous matrix

The 0.2 g of diol moieties modified SBA-15 was dispersed into slightly excessive 5 mM $HAuCl_4$ (Wako) aqueous solution in a beaker with vigorous stirring. Five minutes later, the beaker was placed in the center of a microwave oven with power of 700 W and frequency of 2450 MHz. After 45 s of MR, the mixture solution became purple. After radiation for another 15 s, the solution became wine-red and the radiation was ceased. The resultant suspension was filtered and the residue was washed with water and ethanol and dried to get the Au/SBA-15. The 0.2 g of SBA-15 with amino-group modified was also dropped into the $HAuCl_4$ aqueous solution under otherwise the same procedure as performed for diol-group modified MMs, which served as control and contrast experiments.

The unsupported gold nanoparticles were obtained by dissolving the silica frameworks with a solution of HF/H_2O/ethanol added with alkanethiols as a stabilizing ligand [1]. Typically, 0.1 g of Au/SBA-15 was dispersed in 20 mL of ethanol containing 0.8 g of 1-dodecanethiol ($C_{12}H_{25}SH$, Wako). The silicate host was etched by adding 5 mL of aqueous HF (4%, Wako) solution to the dispersion with sonication for 40 min. After centrifugation, a light wine-red supernatant was discarded and the precipitate was rinsed carefully with the mixture of ethanol and water. The washed precipitate was then dispersed in tetrahydrofuran, resulting in dark wine-red solution.

2.4. Characterization

X-ray diffraction (XRD) patterns were collected with M03X-HF22 X-ray diffractometer using Cu$K\alpha$ radiation (40 kV, 40 mA, $\lambda = 1.5418$ Å). High-resolution transmission electron microscopy (HRTEM), selected area electron diffraction (SAED) and energy-dispersive spectroscopy (EDS) were conducted with JEOL 200CX electron microscope operated at 200 kV. The TEM samples were prepared by mixing the powder with ethanol, and depositing them onto a holey carbon film on a Cu grid. UV–vis absorption spectra were recorded on a Shimadzu UV–vis 3101 spectroscopy. N_2 adsorption and desorption isotherms were measured at 77 K on Autosorb-1 system. The specific surface area and the pore size distribution were calculated using the BET and Barrett–Jonyner–Halenda (BJH)

methods, respectively. Solid-state ^{13}C cross-polarization magic angle spinning (CP/MAS) NMR spectra were recorded on JEOL CMX-300 spectrometer. The conditions for the measurement are an acquisition time of 102.4 ms, a contact time of 5.0 ms, and a pulse delay of 15.0 s.

3. Results and discussion

Microwave is a portion of the electromagnetic spectrum with frequencies in the range of 300 MHz–300 GHz. The commonly used frequency is 2.45 GHz. In the microwave frequency range, polar molecules such as ethylene glycol (EG) try to re-orientate with respect to an alternating electric fields, consequently lose energy by molecular friction, and result in volumetric heating [26,27]. The degree of interaction of microwave with a dielectric medium is related to the material's dielectric and dielectric loss constants. Among the chemicals, EG have high dielectric and dielectric loss constants and hence a high microwave activation [25,26]. Therefore, EG could be heated rapidly and selectively under MR. The fast heating by microwave accelerates the reduction of the metal precursor and the homogeneous nucleation and growth of metal particles. Generally, EG could act as reducing centers to reduce metal ions to their zero oxidation state by the following mechanism [28,29]:

$$CH_2OH - CH_2OH \xrightarrow{MR} CH_3CHO + H_2O,$$

$$2nCH_3CHO + 2M^{n+} \rightarrow 2M + 2nH^+ + nCH_3COCOCH_3.$$

Based on the above mechanisms, we propose this new synthetic protocol for the preparation of highly dispersed gold nanoparticles within the pore channels of mesoporous silica as shown in Scheme 1. Using APS to react with Si–OH groups on the internal pore surfaces of MMs, the basic $-NH_2$ moieties could be effectively grafted on the mesochannels of SBA-15 [31]. A subsequent simple addition reaction between $-NH_2$ groups and glycidol will introduce diol groups into the pore channels [32], which will be served as active sites for the reduction of the metallic precursors upon MR.

The assembly procedures of diol moieties in the synthesized SBA-15 were monitored by solid-state NMR spectroscopy as shown in Fig. 1. No observable carbon signal is detected for the as-synthesized MMs (data not shown), indicating that the surfactant was totally removed by the extraction process employed. After modification of amino groups, three clear resonance peaks at δ values of

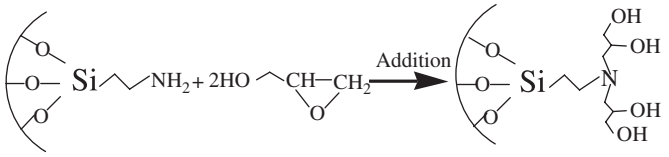

Scheme 1. The designed protocol to introduce diol moieties for the reduction of metallic nanoparticles upon MR.

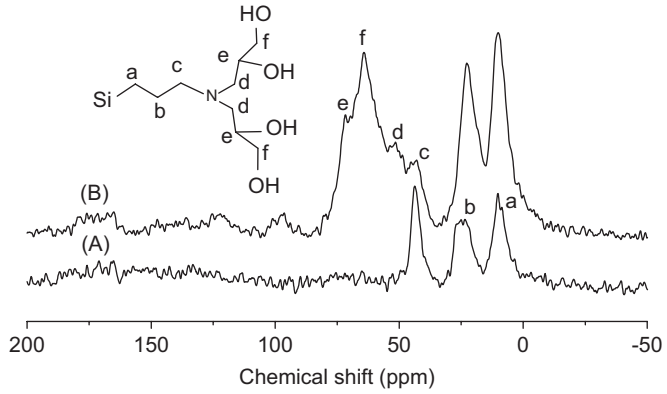

Fig. 1. Solid-state ^{13}C CP/MAS NMR spectra of the SBA-15 mesoporous materials: (A) modified with organic amino groups and (B) modified with diol moieties.

10.2 ppm (Si–CH_2), 23.8 ppm (Si–CH_2–CH_2) and 42.6 ppm (–CH_2–NH_2) are observed (Fig. 1A), which demonstrates that organic amino-group is successfully grafted onto the surface of MMs [33]. Peaks are relatively broad attributed to the restricted mobility of the functional groups attached to the surface of SBA-15 [34]. After a simple addition reaction between amino groups and glycidol, three new resonance peaks at 51.2, 64.2 and 71.9 ppm appear, which are assigned to *d*, *f*, and *e* position carbons [35] as shown in Fig. 1B, respectively. On the basis of the ^{13}C CPMAS NMR spectra, the diol moieties are effectively grafted onto the framework of mesoporous SBA-15, which will serve as reduction centers for the gold nanoparticles precursors. The resonance peaks assigned to diol moieties could not be removed by repeated washing, also suggesting that they are firmly entrapped in the silicate matrix by covalent links.

MR reduction reaction was tracked by UV–vis. Before MR, the mixture aqueous solution of $HAuCl_4$ and SBA-15 modified with diol moieties shows two intense charge transfer bands, peaking at 212 and 234 nm, and a moderate *d–d* transition band at around 310 nm as shown in the inset of Fig. 2 [31]. After 45 s of MR, the yellow mixture solution in a beaker became purple, suggesting that the nucleation and growth speed of gold nanoparticles were rapid. After 60 s of radiation, the solution became wine-red and the radiation was ceased. Fig. 2 shows the UV–vis spectra of SBA-15 with the diol moieties modified and the Au/SBA-15 composite MMs. From Fig. 2a, SBA-15 with diol moieties assembled shows no absorption in the wavelength region >400 nm, the Au/SBA-15 composite MMs reveals a surface plasmon resonance (SPR) absorption peak at ca. 528 nm as shown in Fig. 2b. The SPR indicates that the gold particles are not only formed but also ranged in nano-scale [1,21]. Since the Au/SBA-15 is visually red in solid form or when dispersed in solution, it should not contain a nanoparticle aggregate with typical color of blue-purple [36]. No peak in the near-IR region also rules out the presence of nanorods [37]. Since MR was immediately ceased upon the termination of reduction of gold nanoparticle precursor, no further growth is expected;

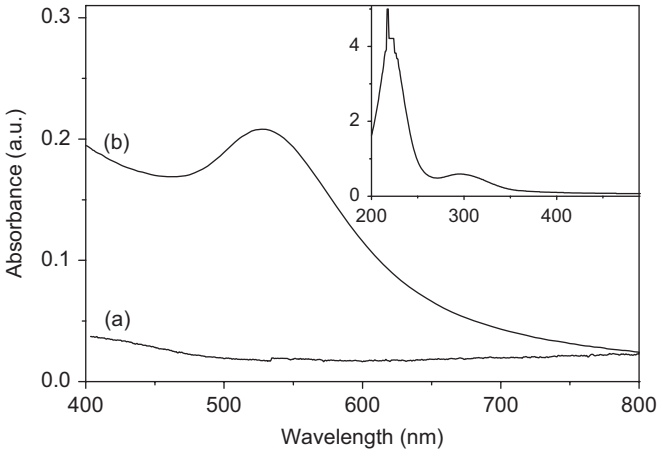

Fig. 2. UV–vis absorption spectra of (a) mesoporous SBA-15 with diol moieties modified and (b) composite mesoporous silica with gold nanoparticles loaded. The inset shows the UV–vis absorption of $HAuCl_4$ aqueous solution mixed with diol modified mesoporous SBA-15 before MR.

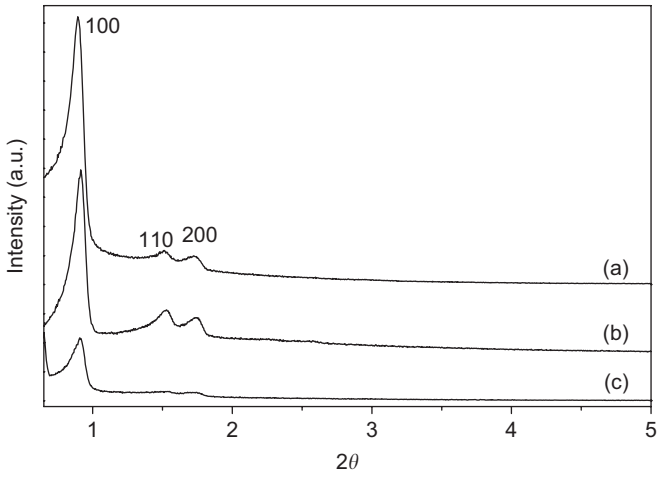

Fig. 3. Small angle XRD patterns of: (a) as prepared mesoporous silica; (b) mesoporous silica with diol moieties grafted after removal of surfactant; and (c) mesoporous silica with highly dispersed gold nanoparticles loaded.

therefore, it is reasonably concluded that the dimension can be controlled in the form of nanoparticles. This UV–vis analysis gives a primary concept that MR combining with SBA-15 template could effectively mediate the size and dimension of the synthesized gold nanoparticles. We also performed control experiments. When the SBA-15 with amino-groups modification was dropped into the $HAuCl_4$ aqueous solution, no color change for the solution and no SPR peak for the sample were observed even upon MR for several minutes. Meanwhile, if no MR was applied to the mixture for the sample preparation, no SPR peaks or color changes were observed. All these phenomena agree well with a fact the MR is necessary and efficient for the synthesis of Au/SBA-15.

Mesostructural and ordered characteristics of the mesoporous SBA-15 were manifested by XRD measurements. Fig. 3a–c correspond to small angle XRD patterns of the as prepared SBA-15, mesoporous silica with diol moieties and the Au/SBA-15, respectively. All of these patterns show 100, 110 and 200 reflections, which are characteristic of a two-dimensional hexagonal (*p6mm*) structure [7]. The existence of the main diffraction peaks illustrates that the framework hexagonal ordering of SBA-15 has been retained very well after the functionalization treatment as well as gold incorporation. After the extraction and modification of SBA-15, the peaks shift toward the higher angle region due to the further contraction of silica framework [1]. An apparent decrease of the small angle XRD peak intensity can be found after the incorporation of gold nanoparticles in consistent with the reported results [31], which maybe results from the reduction of contrast between pore channels and walls due to the pore filling of Au. The main diffraction peak at *d*-spacing of $d_{100} = 9.63$ nm for Au/SiO_2 corresponds to a hexagonal cell parameter $a = 11.1$ nm. The presence of characteristic diffraction peaks at $2\theta = 38^\circ$, assigned to

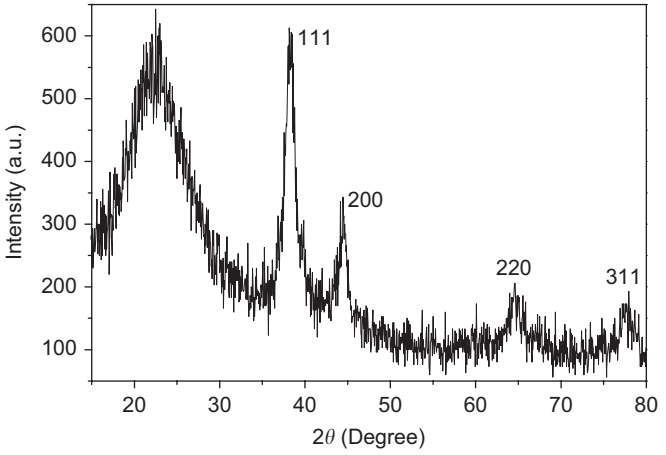

Fig. 4. The wide angle XRD patterns of mesoporous silica with gold nanoparticles loaded.

(111) planes of the face-centered cubic (fcc) structure of gold, indicates that gold nanoparticles has crystallized as shown in Fig. 4. The other peaks pertained to (200), (220) and (311) can also be clearly visualized. The small crystalline grain sizes, resulting from the confined growth of gold within the mesoporous channels, can cause the broadened diffraction peaks. According to the Scherrer formula [38] of $d = k\lambda/\beta_{1/2}\cos\theta$, the mean diameter of gold nanoparticles is calculated to be 7.9 nm, where the $\beta_{1/2}$ is the full-width at half-maximum of the peak at 2θ, k is a constant of 0.89 and λ is the wavelength of Cu$K\alpha_1$ radiation.

The N_2 adsorption and desorption isotherms for the synthesized mesoporous silica, SBA-diol and the Au/SBA-15 composite MMs are shown in Fig. 5. All of the isotherms are of type IV classification, which is typical of adsorption of SBA-15. A well-defined step occurs approximately at a relative pressure p/p_0 of 0.6–0.8, associated with the filling of the mesopores due to capillary

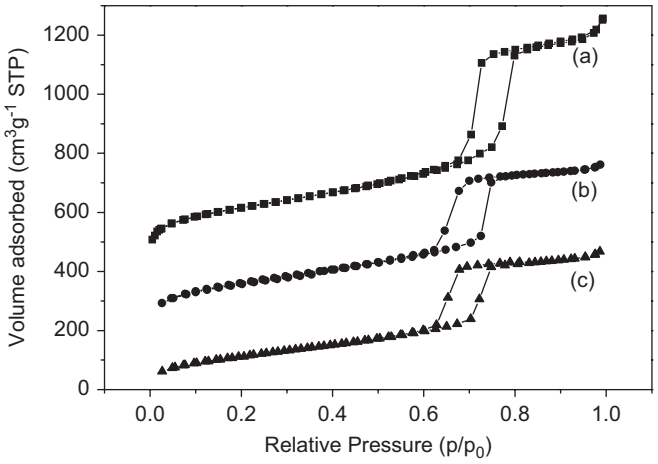

Fig. 5. Nitrogen adsorption–desorption isotherm for: (a) the synthesized mesoporous silica without surfactant; (b) mesoporous silica with diol modified; and (c) the composite mesoporous materials with gold nanoparticles loaded.

Table 1
Pore structure parameters of: (A) the synthesized mesoporous silica without surfactant, (B) mesoporous silica with diol modified and (C) the composite mesoporous materials with gold nanoparticles loaded

Samples	A_{BET} (m^2/g)	V_{BJH} (cm^3/g)	D_{BJH} (nm)	d_{100} (nm)	A_0 (nm)
A	751	1.32	8.9	9.9	11.4
B	425	0.78	7.9	9.6	11.1
C	225	0.62	7.8	9.6	11.1

A_{BET}: BET surface area, V_{BJH}: BJH total pore volume, D_{BJH}: BJH pore diameter, d_{100}: plane separation distance, $A_0 = 2d_{100}/3^{1/2}$.

condensation [7]. After formation of gold nanoparticles, the amount of adsorbed nitrogen decreases and the inflection point of the step shifts to a smaller p/p_0. The reduced amount of nitrogen adsorption is caused by a smaller specific surface, while the shift of the step to lower relative pressure is indicative of smaller pore sizes. The BET surface area of SBA-diol is 425 m^2/g and decreases down to 225 m^2/g for the sample with gold nanoparticles loaded. The pore volume also decreases in a similar way. This decrease is consistent with a large portion of the pore volume being occupied by the gold nanoparticles. Au/SiO_2 composite MMs still show mesoporosity, suggesting that gold nanoparticles are dispersed throughout the whole channels and the mesoporous channels are still maintained [39]. The pore structure parameters of samples are summarized in Table 1.

The morphology and distribution of Au within the pore channels of SBA-15 were directly observed by TEM. From Fig. 6a, the highly ordered hexagonal pore structure of SBA-15 is maintained during the formation of gold nanoparticles in agreement with the above SAXRD results. It can be observed that uniformly and highly dispersed Au nanoparticles as dark dots have been exclusively confined in the hexagonal channels. No bulk aggregation of the gold metal on the outer surface could be found, which indicates that MR rapid synthesis route could effectively avoid the problems caused by traditional wet impregnation method. The Au nanoparticles are in the size range of 5–10 nm, and no nanorods or nanowires are present, which is consistent with the analysis of UV–vis. The particle size from TEM

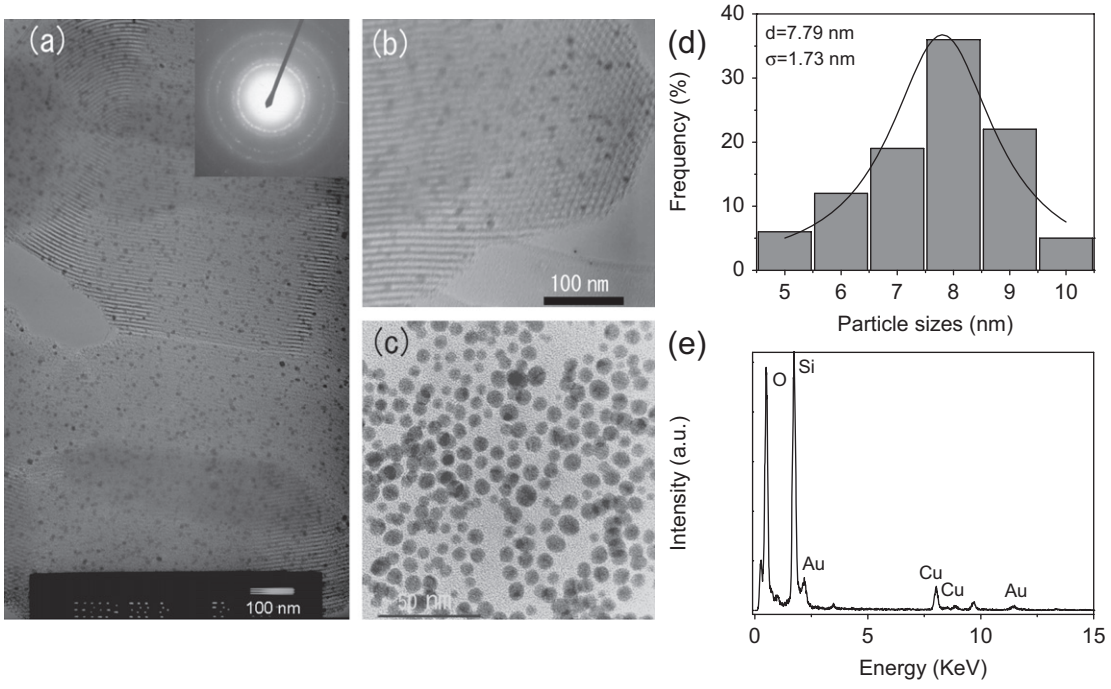

Fig. 6. Typical TEM images of the composite mesoporous silica filled with gold nanoparticles: (a) total image viewed along the direction paralleled to mesochannels and the inset shows the corresponding selected area electron diffraction; (b) a local magnified image viewed along the direction perpendicular to the mesochanneals; (c) an image of unsupported gold nanoparticles after the removal of the mesoporous framework by $C_{12}H_{25}SH$/HF/ethanol mixing aqueous solution; (d) the histogram with Gaussian curve fitted to the data for the analysis of the gold nanoparticle size distribution after SBA-15 matrix removal corresponding to Fig. 6c; and (e) EDS spectrum of gold content within SBA-15 corresponding to Fig. 6a.

observation also agrees well with the results of XRD measurements. In the SAED pattern as shown in the inset of Fig. 6a, diffraction rings/spots are observed that are indexed to (111), (200), (220), and (311) reflections of fcc Au, indicating that the gold nanoparticles are crystallized in agreement with the results of XRD. The simultaneous EDS in Fig. 6e reveals that the gold contents have almost no difference with the direction of incident electron beams, which further indicates that uniformly and highly dispersed gold nanoparticles are obtained in the hexagonal channels. For the current sample observed, the corresponding gold weight content is about 9%.

A local magnified image viewed along the direction perpendicular to the mesochannals is also presented in Fig. 6b, which further reveals the highly homogeneous distribution of the gold nanoparticles in the mesoporous silica matrix. Extraction of the gold nanoparticles from SBA-15 matrix results in milligram quantities of gold nanoparticles with low dispersity as shown in Fig. 6c. The resulting particles are 5–10 nm in diameter with average particle size of ca. 8 nm in agreement with the results of XRD measurements. The detailed size distribution analysis is present from histogram in Fig. 6d. Gaussian curve fit and statistic analysis give a mean particle diameter of 7.8 nm and standard deviation of 1.7 nm, which is less polydisperse (ca. $\pm 20\%$) than those obtained via the conventional solution synthesis (typically $\pm 30\%$) [17]. This particle size is also comparable with the pore size by BJH calculation, further demonstrating the template effect by parent SBA-15 matrix. Obviously, this rapid and efficient method provides a scale-up route for the production of gold nanoparticles with low dispersion.

4. Conclusions

In summary, a facile and novel strategy has been developed to incorporate gold nanoparticles into the pore channels of mesoporous SBA-15 assisted by MR. Inherent advantages of this strategy are its mild reaction condition and rapid reaction speed. Low-temperature process avoids the aggregation of the nanoparticles at the entry or outer surface of mesoporous SBA-15. Selective microwave absorption by diol moieties facilitates the synthesis of gold nanoparticles rapidly within tens of seconds. Due to the rapid and homogeneous nucleation, simultaneous propagation and termination of reaction by MR, the size of gold nanoparticles is effectively controlled. Extraction of the entrapped gold from the nanocomposite results in milligram quantities of gold nanoparticles with low dispersity. This rapid and efficient method provides a scale-up route for the production of gold nanoparticles. It is obvious that this route can be applied to the other metals through the selection of proper metallic precursors. Further works are being carried out on other nanoparticles and the applications of the synthesized mesoporous silica with metallic nanoparticles incorporated.

Acknowledgments

This work was supported by the Japan Society for the Promotion of Science (JSPS). We also give our thanks to Dr. Qing Huang from National institute for Materials Science in Japan and Dr. Toshiyuki Yokoi and Prof. Takashi Tatsumi from the Tokyo Institute of Technology for providing several characterization equipments.

References

[1] J.L. Gu, G.J. You, J.L. Shi, L.M. Xiong, Z.L. Hua, H.R. Chen, S.X. Qian, Adv. Mater. 17 (2005) 557.
[2] Z.Y. Zhong, J.Y. Lin, S.P. Teh, J. Teo, F.M. Dautzenberg, Adv. Funct. Mater. 17 (2007) 1402.
[3] C.K. Tsung, W.B. Hong, Q.H. Shi, X.S. Kou, M.H. Yeung, J.F. Wang, G.D. Stucky, Adv. Funct. Mater. 16 (2006) 2225.
[4] Y. Xia, P. Yang, Y. Sun, Y. Wu, B. Mayers, B. Gates, Y. Yin, F. Kim, H. Yan, Adv. Mater. 15 (2003) 353.
[5] D. Walsh, L. Arcelli, T. Ikoma, J. Tanaka, S. Mann, Nat. Mater. 2 (2003) 386.
[6] A.H. Lu, F. Schuth, Adv. Mater. 18 (2006) 1793.
[7] D. Zhao, J. Feng, Q. Huo, N. Melosh, G.H. Fredrickson, B.F. Chmelka, G. D Stucky, Science 279 (1998) 548.
[8] Y. Wan, H.F. Yang, D.Y. Zhao, Acc. Chem. Res. 39 (2006) 423.
[9] J.L. Shi, Z.L. Hua, L.X. Zhang, J. Mater. Chem. 14 (2004) 795.
[10] M. Bandyopadhyay, O. Korsak, M.W.E. Van den Berg, W. Grunert, A. Birkner, W. Li, F. Schuth, H. Gies, Microporous Mesoporous Mater. 89 (2006) 158.
[11] H.R. Chen, J.L. Shi, Y.S. Li, J.N. Yan, Z.L. Hua, H.G. Chen, D.S. Yan, Adv. Mater. 15 (2003) 1078.
[12] A.Q. Wang, C.M. Chang, C.Y. Mou, J. Phys. Chem. B 109 (2005) 18860.
[13] C. Aprile, A. Abad, G.A. Hermenegildo, A. Corma, J. Mater. Chem. 15 (2005) 4408.
[14] M.Y.Y. Chen, J.S. Qiu, X.K. Wang, J.H. Xiu, J. Catal. 242 (2006) 227.
[15] G. Gupta, P.S. Shah, X.G. Zhang, A.E. Saunders, B.A. Korgel, K.P. Johnston, Chem. Mater. 17 (2005) 6728.
[16] P. Botella, A. Corma, M.T. Navarro, Chem. Mater. 19 (2007) 1979.
[17] T. Asefa, R.B. Lennox, Chem. Mater. 17 (2005) 2481.
[18] P. Botella, A. Corma, M.T. Navarro, Chem. Mater. 19 (2007) 1979.
[19] J.L. Gu, J.L. Shi, L.M. Xiong, H.R. Chen, M.L. Ruan, Microporous Mesoporous Mater. 74 (2004) 199.
[20] A. Fukuoka, T. Higuchi, T. Ohtake, T. Oshio, J. Kimura, Y. Sakamoto, N. Sugimoto, S. Inagaki, M. Ichikawa, Chem. Mater. 18 (2006) 337.
[21] J.L. Gu, L.M. Xiong, J.L. Shi, Z.L. Hua, L.X. Zhang, L. Li, J. Solid State Chem. 179 (2006) 1060.
[22] L.Z. Wang, J.L. Shi, W.H. Zhang, M.L. Ruan, J. Yu, D.S. Yan, Chem. Mater. 11 (1999) 3015.
[23] M.H. Huang, A. Choudrey, P.D. Yang, Chem. Commun. (2000) 1063.
[24] L.X. Zhang, J.L. Shi, J. Yu, Z.L. Hua, X.G. Zhao, M.L. Ruan, Adv. Mater. 14 (2002) 1510.
[25] M. Tsuji, N. Miyamae, M. Hashimoto, M. Nishio, S. Hikino, N. Ishigami, I. Tanaka, Colloid Surf. A 302 (2007) 587.
[26] M. Tsuji, M. Hashimoto, Y. Nishizawa, M. Kubokawa, T. Tsuji, Chem. Eur. J. 11 (2005) 440.
[27] W.X. Chen, J.Y. Lee, Z.L. Liu, Chem. Commun. (2002) 2588.
[28] M.S. Rahuveer, S. Agrawal, N. Bishop, G. Ramanath, Chem. Mater. 18 (2006) 1390.
[29] J.F. Zhu, Y.J. Zhu, J. Phys. Chem. B 110 (2006) 8593.
[30] B.Z. Tian, X.Y. Liu, C.Z. Yu, F. Gao, Q. Luo, S.H. Xie, B. Tu, D.Y. Zhao, Chem. Commun. (2002) 1186.

[31] J.L. Gu, J.L. Shi, Z. Hua, L.M. Xiong, L.X. Zhang, L. Li, Chem. Lett. 34 (2005) 114.
[32] H. Mori, A.H.E. Muller, J.E. Klee, J. Am. Chem. Soc. 125 (2003) 3712.
[33] J.L. Gu, W. Fan, A. Shimojima, T. Okubo, Small 3 (2007) 1740.
[34] S. Sadasivan, D. Khushalani, S. Mann, J. Mater. Chem. 13 (2003) 1023.
[35] J. Ding, C.J. Hudalla, J.T. Cook, D.P. Walsh, C.E. Boissel, P.C. Iraneta, J.E. O'Gara, Chem. Mater. 16 (2004) 670.
[36] R. Elghanian, J.J. Storhoff, R.C. Mucic, R.L. Letsinger, C.A. Mirkin, Science 277 (1997) 1078.
[37] L.F. Gou, C.J. Murphy, Chem. Mater. 17 (2005) 3668.
[38] G.J. Wilson, A.S. Matijasevich, D.R.G. Mitchell, J.C. Schulz, G.D. Will, Langmuir 22 (2006) 2016.
[39] F. Gao, Q. Lu, X.Y. Liu, Y.S. Yan, D.Y. Zhao, Nano Lett. 1 (2001) 743.